Continuous vs. Discontinuous Crack Extension: Characterization of Ductile Tearing in Thin Plates

Volodymyr P. Naumenko*

Department of Structural Integrity, G. S. Pisarenko Institute for Problems of Strength, Kyiv 01014, Ukraine;
E-mail: v.p.naumenko@ipp.kiev.ua

Abstract There are two alternative trends of thought concerning the mechanism of crack extension in an elastic-plastic material subjected to monotonically and slowly increasing tensile (Mode I) loading. The crack advances continuously, by infinitesimal growth steps, or discontinuously in finite growth steps. In this experimental study, slant cracks were extended in thin aluminium plates, depending on theirs geometry, with or without an intermittent attainment of the local instabilities displayed in test records. It means that the mechanism of ductile tearing in the test material may be changed simply by changing the specimen geometry. This observation is not in accord with the well-known energetic considerations that a mechanism of crack extension in a non-hardening or low-hardening elastic-plastic material must be only discontinuous. A wide consensus exists that a single-parameter characterization of crack extension is conceptually possible when fracture resistance is quantified by a critical, lower-limiting value ψ_c of the Crack Tip Opening Angle (CTOA-ψ). It is of scientific and practical interest to measure CTOA-ψ for slant cracks growing at different in-plane constraint states and in this way to clear up the above contradiction. In our specimens that were fractured under the highly constrained conditions of transverse plane strain, cracks were advancing in well-defined steps.The CTOA- ψ values related to different pairs of distinct fracture events strongly depend upon the choosing the neighboring pair. They were compared with the critical angles ψ_c determined with the use of ASTM/ ISO Standard test method and also with the CTOA-ψ_n values established from profiles of fully-developed cracks.

Keywords Crack extension, Thin plates, Thin-sheet aluminium, Crack tip opening angle, In-plane constraint

1. Introduction

There is an increasing interest in the development of valid fracture criteria and standard test methods for unified assessment of ductile tearing in thin-wall components. This paper deals with the characterisation of plane stress tearing under uncontained yielding in rectangular plates (Fig. 1) made from thin sheets of a high-strength low-hardening aluminium alloy. The principal obstacle to the development of an easy-to-use procedure for assessing the resistance to stable crack extension is placed by the need to correlate too many variables governing the fracture behaviour in ductile materials. These are the parameters of elasticity, including those of out-of-plane deformation (buckling); plasticity, including those of residual stress effects and anisotropy; diffused and localised necking; damage and cracking. It seems highly improbable to predict fracture using only the near crack-tip parameters in isolation from the global deformation pattern.

Therefore, in collecting test data a purely mechanistic approach based on the minimum of assumptions was adopted. In this way, our concept of through-life fracture assessment [1-7] attempts to formalize the characterization of crack extension using only the interrelations between directly measurable quantities without taking into account the physical damage mechanisms in vicinity of a fracture process zone. Here, the term *through-life assessment* means that all measures of tear resistance can be determined continuously (from the nucleation of a tear crack and up to the complete separation) or in a point-by-point manner for test events of practical importance.

We suggest that the global fracture behavior expressed in terms of averaged quantities might be assessed immediately from diagrams of loads vs. displacements vs. distances between the extreme

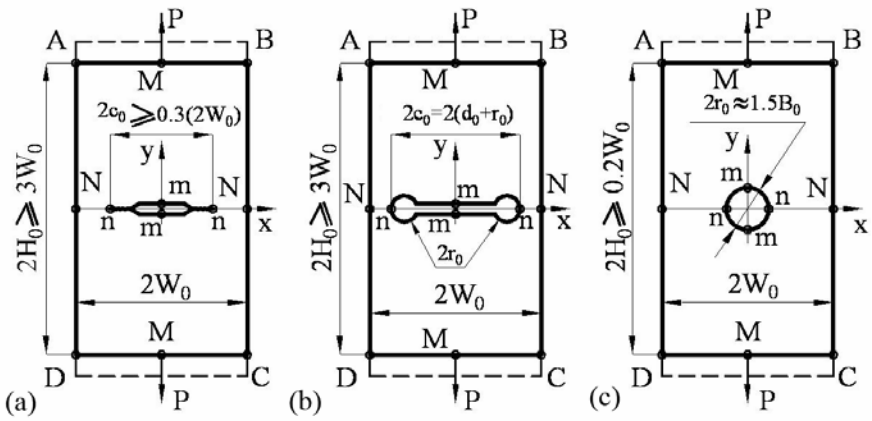

Figure 1. Geometry of the standard M(T) specimen containing initial fatigue pre-cracks at a slot tips (a) and MDR(T) (b) and MR(T) (c) specimens with simple and well-defined geometry of an original stress raiser.

points on a specimen surfaces. These are (Fig. 1) the points *m* and *n* on the inner and *M* and *N* on the outer boundaries of a specimen Problem Domain (PD). The emphasis is on experimental investigation into the effects of such constraint-related issues as geometry and size of the PD containing an original stress raiser of a relatively small size (Fig 1c).

To trigger the progressive process of single-site necking followed by single-site cracking in a predetermined location and direction, a variety of imperfections are employed in plane-stress fracture studies. According to the standard test methods [8-10], the specimen should contain initial fatigue precracks at the tips of a starting stress raiser (Fig. 1a). However, it is common knowledge that the crack extension resistance in metallic materials may be influenced significantly by the preloading history. At present, there is no possibility to establish a one-to-one correspondence between the initial fatigue damages near the crack tips in different specimens whose geometry, loading and boundary restraints vary over wide ranges.

That is why in the specimen preparation, special care must be taken to prevent the introduction of uncontrollable initial damages and residual stresses into the material to be tested. In our approach [1-7], tests are carried out on specimens with an original stress raiser having relatively simple geometry and a well-defined form of its tips (points *n* in Figs 1b and 1c). By convention, the specified open hole is taken as a damage-free defect. Its diameter $2r_0$ should be sufficiently small in comparison with the PD dimensions $2W_0$ and $2H_0$. It means that at the instant of fracture initiation the tensile stress σ averaged across the specimen ligament depends only slightly on the variation in the hole radius r_0. At the same time, the original stress raiser should be sufficiently large to concentrate all thinning and structural damage inside a single localised neck.

Constraint-related issues such as original geometry and size of the outer and inner boundaries of a MDR(T) and MR(T) specimens (Fig. 1) are investigated experimentally. The focus is on revealing the distinctions between the characteristic values of the CTOA-ψ associated with the fully-controllable pop-in fracture behaviour and those determined with the use of ASTM/ ISO Standard test method [9, 10]. This method applies specifically to fatigue pre-cracked M(T) and C(T) specimens that exhibit low constraint and are tested under slowly increasing displacement. Here and then, we deal only with the M(T) geometry (Fig. 1a) originally introduced in standard [8]. The angle ψ_c generated following the procedure and a guideline contained in standards [9, 10] is treated as insensitive to in-plane dimensions and specimen type, but is dependent upon specimen thickness. In other word, the lower-limiting value ψ_c of CTOA-ψ can be used in analyses of stable crack extension as a quantity that is independent on a level of the global in-plane constraint.

The problem under consideration is addressed in two parts. We start with comparing the profiles of fully-developed tear cracks in broken-down MR(T) and MDR(T) specimens of different geometries and size. The intent is to demonstrate a need for incorporating in current practice of testing and analysis the notion *reference level of resistance to stable crack extension*. In the second part of this work, test records with orderly dips on theirs softening branches are presented and discussed. The objective is to contrast the concepts of continuous and continuous crack extension by comparing the crack profiles generated in a course of actual and virtual enlargements of a crack cavity volume.

2. Material and Tests

The test material is aircraft-skin aluminium alloy D16AT in as-received condition, having the form of 1.4-1.5mm thick sheets. Its chemical composition and mechanical properties are close to those of AL 2024-T3. Two sets of standard tensile test specimens of width $2W_0$ = 12mm were loaded under quasi-fixed grip conditions in tension across and along the rolling direction of the sheets. The elastic and anisotropic plastic behaviour f the material was characterized by the following parameters: the elastic modulus E = 68 and 67GPa, Poisson's ratio ν = 0.32, the 0.2% offset yield strength σ_{02} = 299.4 and 338MPa, and the ultimate tensile strength σ_{UTS} = 446 and 467MPa, respectively.

The uniaxial crack extension tests were performed on MDR(T) and MR(T) specimens of large and small width $2W_0$ with stress raisers of various shapes and sizes given in Table 1. The horizontal boundaries of each PD were rigidly clamped. In the tests to separation failure, they were moving with a sufficiently small rate 0.001mm/s, i.e., under the quasi-fixed grip condition. At this rate tear crack extension in the MR(T)-1.0-1.0 specimens with square PD of width $2W_0^{BS}$ =120 mm reproducibly occurs by an intermittent attainment of the local instabilities [4].

Table 1. Principal dimensions of specimens.

Specimen code [a]	$2W_0$ (mm)	$2H_0$ (mm)	$2r_0$ (mm)	$2d_0$ (mm)	$2s(\mathrm{m})_0$ (mm)	$2c_0$ (mm)
1. Small width specimens						
MR(T)-0.5-10.0	1200	600	2	0	2	2
MDR(T)-0.5-10.0	1200	600	2	10	0.12	12
MDR(T)-0.5-10.0	1200	600	2	20	0.12	22
MDR(T)-0.5-10.0	1200	600	2	38	0.12	40
MDR(T)-0.5-10.0	1200	600	2	58	0.12	60
2. Large width specimens						
MR(T)-5.0-1.0	120	600	2	0	2	2
MR(T)-1.5-1.0	120	180	2	0	2	2
MR(T)-1.0-1.0	120	120	2	0	2	2
MDR(T)-1.0-1.0	120	120	2	3	0,12	5
MDR(T)-1.0-1.0	120	120	2	8	0,12	10
MDR(T)-1.0-1.0	120	120	2	18	0,12	20
MDR(T)-1.0-1.0	120	120	2	38	0,12	40
MR(T)-0.1-1.0	120	12	2	0	2	2

[a] The numerical values in the specimen code denote the shape ratio (H_0 / W_0) and the scale ratio (W_0 / W_0^{BS}). In this work we take $2W_0^{BS}$ = 120mm for the MR(T)-0.1-1.0 specimen treated as the basic geometry.

It should be emphasized that in all specimens under consideration tearing occurred by cracking parallel to the rolling direction in the plane inclined at 45° to the specimen surfaces. The regime of slant tearing starts from the very instant *i*0 of crack nucleation and continued up to the complete separation of a specimen by a growing crack at the instant *f* (Figs 2 and 3). Note that sudden formation of two short cracks near the points *n* (Fig. 1) was always preceded by a clearly distinct drop in test records at the attaining the state *t*0 (see Fig. 3b). As can be seen from Fig. 2, the decrease of PD height $2H_0$, when accompanied by the decrease of stress raiser length $2c_0$, ensure realization of the fully-controllable discontinuity of the slant crack extension process [7].

Very orderly dips on the softening branch of the diagram reflect a cyclic variation in the crack profile geometry. Each cycle consists of five test events (Figs 3a and 4). Here. $2v$(L) is the displacement of a grips fixture that was measured in a synchronized manner with the crack extension, displacement $2v$(m) of the points *m* (Fig 1) and force *P* (frequency 5 Hz). The diagrams in Figs (2a, 3 and 4) were obtained on the MR(T) specimens tested without the use of anti-buckling guide plates. Buckling of thin plates is a competitive failure mechanism resulting from the elastic compressive stress acting parallel to the crack growth line. Before tests of the MDR(T) specimens (Table 1) they were lightly clamped between two anti-buckling guide plates.

3. Fully-developed crack profiles

Generally, stable crack extension can be seen as interplay of concurrent processes jointly represented by seven through-life fracture curves on the so-called Integrated Fracture Diagram (IFD) [6, 7]. Of these curves, we consider in some detail only a curve describing the geometry of a fully-developed crack in a broken-down specimen. In fact this is one branch (lower-right) out of four branches of a centre crack profile (see Fig 5a). Further on, this branch of a crack, having the key importance for our approach, will be designated as *n*-relationship of the IFD.

The input data for determination of *n*-relationship are distances $2s(x)_n$ between the lower and upper borders of a fully-developed crack (Fig 5a). Of course, at points $x = \pm c_f$ this distances is taken to be zero. By comparing data presented in Figs 6a and 7a, one can find that crack profiles in the specimens of the small and large width are qualitatively similar. An unexpected result is a significant drop in $s(x)_n$ values for the MR(T)-0.5-10.0 specimen containing the shortest stress raiser. This is the single open hole of diameter $2r_0 = 2$mm.

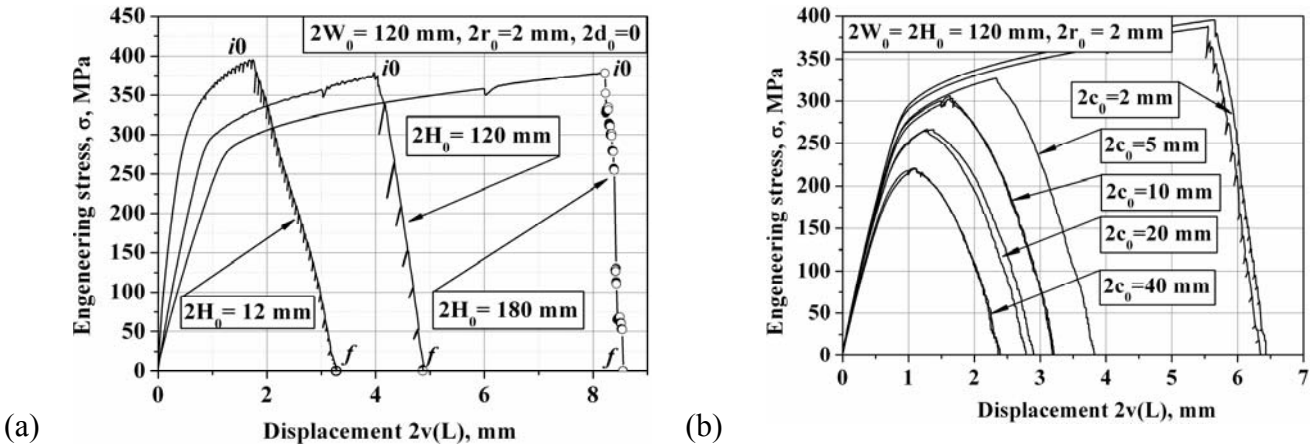

Figure 2. Comparison of test records for the MR(T) specimens of width $2W_0 = 120$mm and different height $2H_0$ (a) shown together with test records for the MDR(T)-1.0-1.0 specimens having the similar PD geometry, but different length $2c_0$ of the original stress raisers with the identical curvature of theirs tips s(b).

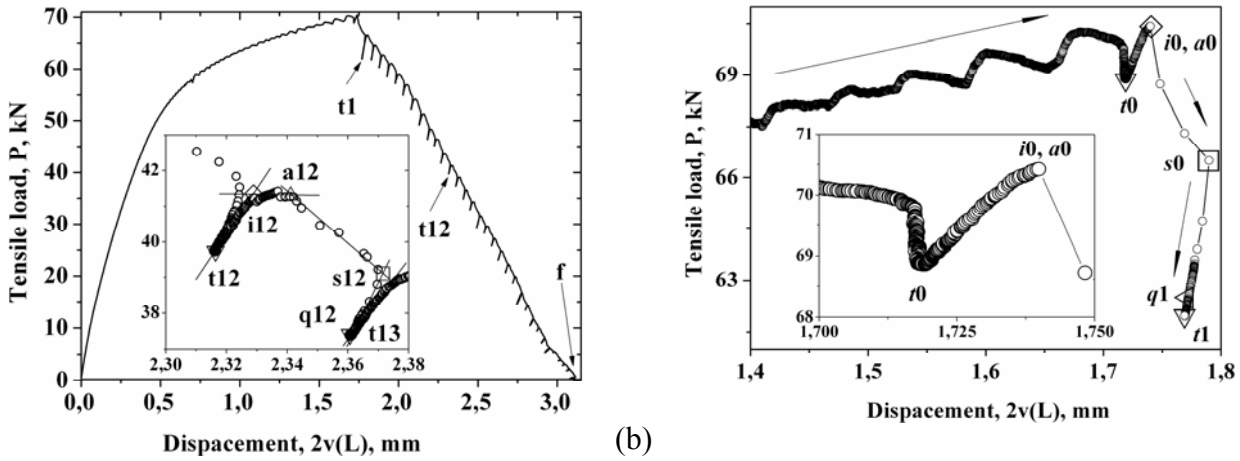

(a) (b)

Figure 3. The enlarged test record that is displayed in Fig. 2a for the MR(T)-0.1-1.0 specimen (a) and its fragment (b) demonstrating that plastic deformation before nucleation of tear cracks and during theirs extension are intrinsically unstable and develops in small temporally confined discontinuous jumps.

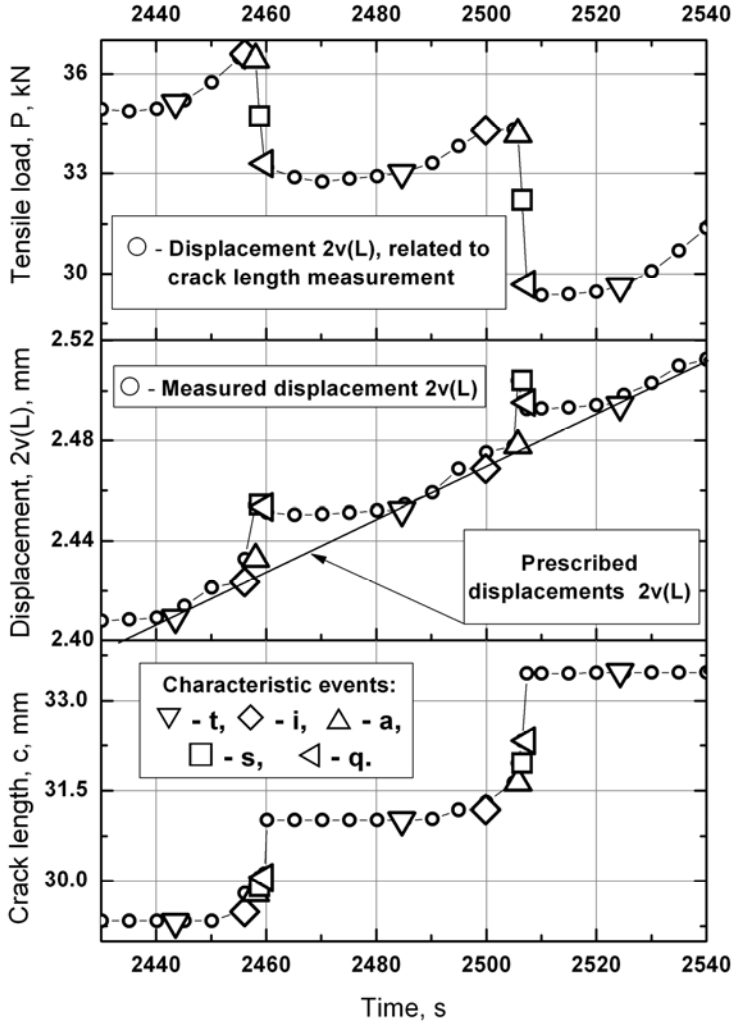

(a) (b) (c)

Figure 4. The timebase fragment of the test-record displayed in Fig. 3a. It is shown together with the related fragment for a synchronized dependence of increments in half-crack length *c* on time.

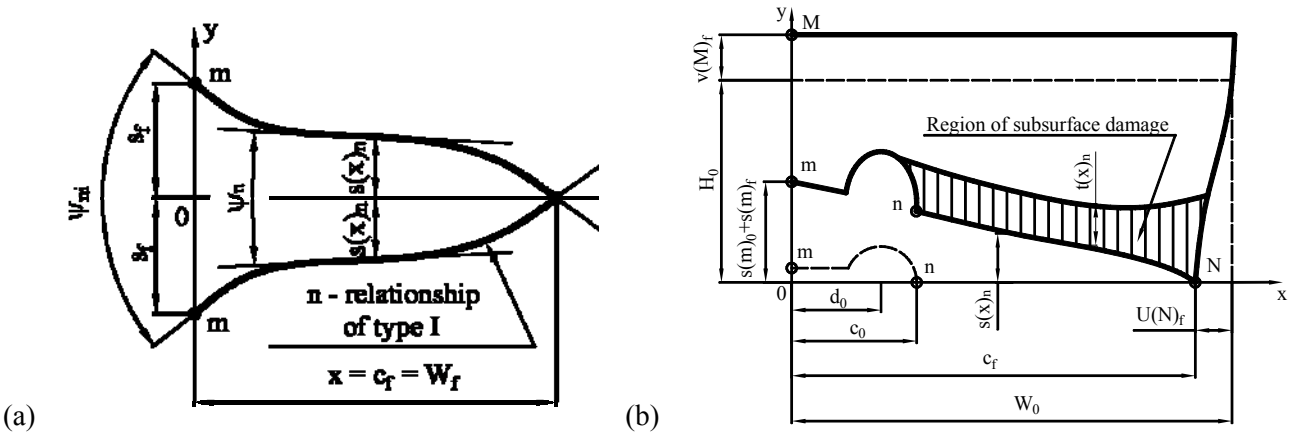

(a) (b)

Figure 5. One-half of an idealized profile for a through-the-thickness crack formed near a point wise imperfection at the centre of a rectangular plate (a) and one-quarter of the MDR(T) problem domain in its initial and broken-down states.

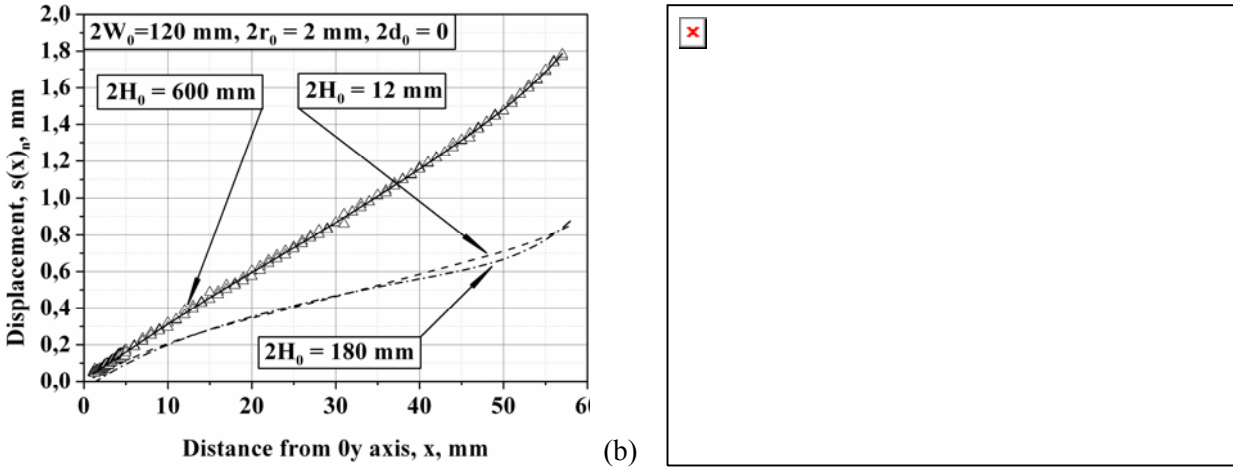

(a) (b)

Figure 6. Through-life fracture curves expressed in terms of the post-test displacements $s(x)_n$ (a) and the post-test values $\psi(x)_n$ of the CTOA-ψ (b) for a set of the MR(T) specimens of the same width with the same hole. These tests were conducted without the use of antibuckling guide plates and without forced unloading.

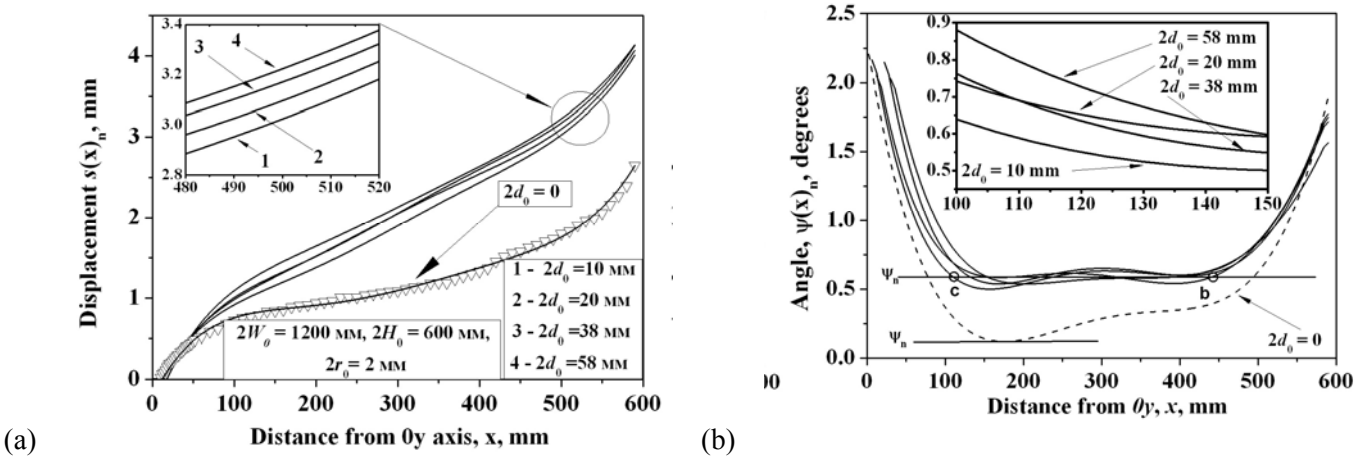

(a) (b)

Figure 7. Through-life fracture curves expressed in terms of the post-test displacements $s(x)_n$ (a) and the post-test values $\psi(x)_n$ of the CTOA-ψ (b) for a set of specimens of the same PD size, but with different stress raisers. These tests were conducted with the use of antibuckling guide plates and without forced unloading.

4. Characterization of ductile tearing resistance

Our displacement-based approach focuses on changes in geometry of the whole crack border, instead of considering mainly the near crack-tip displacements, which are given much attention in the current test procedures [9, 10]. Generally, ductile tearing is seen as interplay of seven processes of continuous (virtual) fracture that are represented by the through-life fracture curves. These latter relate to each other on the IFD by imaginary (instantaneous) unloading-reloading cycles. Such cycles are shown as the straight-vertical lines in Fig. 8 passing through the points *c* and *b* on the *n*-relationship. They bounds the Steady State Tearing (SST) stage, when the plastic component $s(x)_n$ of the virtual crack opening displacement $s(x)$ is in direct proportion to the extension of the virtual crack tips along the 0*x* axis (Fig 1). The virtual crack extension is modelled by continuous moving the upper half of a broken-down specimen towards its lower counterpart, as a rigid body.

Plane stress tearing is considered from the viewpoint of a "moving crack tip" embedded into a fully-developed "moving neck". We assume that the crack surfaces, in their final shape, contain the entire history of accumulating the plastic deformations within the regions of subsurface damage (Fig. 5b). So, there are good reasons for quantifying the resistance to stable crack extension by the plastic component $\psi(x)_n$ of the CTOA-ψ [1-7]. Variations in the value of this angle during the virtual fracture process are determined by the following expression:

$$\psi(x)_n = 2d(s(x)_n)/dx,. \tag{1}$$

Consequently, the simplified assessment of ductile tearing can be performed using only post-test measurements of the virtual crack opening displacement $2s(x)_n$. The tensile testing of the MR(T) specimens (Fig. 1c) is the most promising and practical route to assess effects of constraint on ductile tearing in thin sheets of metallic materials. In this case, the global in-plane constraint can be varied merely by changing the distance $2H_0$ between the rigidly clamped boundaries of a specimen.

Experimental results of this and previous studies [1-7] are contradictory to the commonly accepted statement that the constraint effect in plane stress specimens is negligible. A decrease in the specimen aspect ratio H_0 / W_0 taken together with an increase in the PD width $2W_0$ elevates

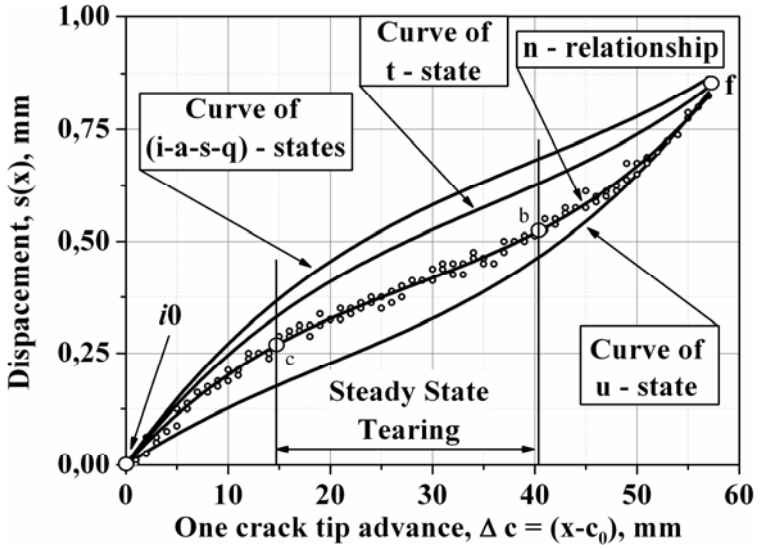

Figure 8. The Integrated Fracture Diagram (IFD) derived from test data for three identical MR(T)-1.0-1.0 specimens of the following dimensions: $2W_0 = 2H_0 = 120$mm, $2r_0 = 2$mm and $2d_0 = 0$. These tests were conducted without the use of antibuckling guide plates and with forced unloading-reloading cycles.

the in-plane constraint (Figs 6b and 7b). These changes are accompanied by the wide variations of the buckling behaviour and crack extension rate [6, 7]. An extremely high level of the global in-plane constraint corresponds to the conditions of transverse plane strain, when in the course of crack extension the outer specimen boundaries $x = \pm W_0$ are straight and fixed ($u(\mathrm{N})_f = 0$ in Fig 5b).

A sufficient level of the proximity to this conditions is achieved in testing the specimens of the basic geometry ($H_0 = 0.1W_0$). In this case, the SST resistance for the Al-alloy D16AT is presented by the angle ψ_n = (1.38 ± 0.1) degrees. This reference value is about half of the lower-limiting value ψ_c = (3.0 ± 1.5) degrees determined for the material in question in [3] with the use of ASTM/ ISO Standard test method [9, 10]. In comparison with the critical angle ψ_c, the novel characteristic of ductile tearing ψ_n is much more consistent and reproducible quantity.

Figures 6b and 7b show that the SST resistance, as measured by the angle ψ_n, contrary to fracture initiation resistance ψ_{ni}, is very sensitive to changing the specimen geometry and size. In the whole, our results [1-7] demonstrate that the CTOA-ψ depends on the combined effects of many variables, namely, PD geometry and its size, geometry and type of an original stress raiser, boundary restraints, buckling behaviour, crack extension rate, as well as technique used for evaluating this fracture parameter. In particular, one can see (Fig. 9) that the angle β associated with the different pairs of distinct fracture events strongly depends upon the choosing a neighboring pair. For the MR(T)-0.1-1.0 specimen of the basic geometry this angle closely correlates with the CTOA- ψ.

Test data for MR(T) specimens give a simple, inexpensive and yet accurate estimations of fracture initiation stress σ_{Ni} for shallow cracks originating from a typical stress raiser. The large distinctions between the lower-limiting values of this stress for the PD of different size observed in Fig. 10 call into question the very meaning of the commonly used characterisation of the net-section stresses in terms of the flow stress $\sigma_f = 0.5(\sigma_{02} + \sigma_{UTS})$. The characteristic values σ_{Nt}, σ_{Ni} and σ_{Ns} of the stress σ_N have the advantage of relating directly to the actual state and position of advancing crack tips. Besides, they relate closely to such customarily quantities as the yield strength σ_{02} and ultimate tensile strength σ_{UTS} obtained under uniform straining of the standard smooth specimens.

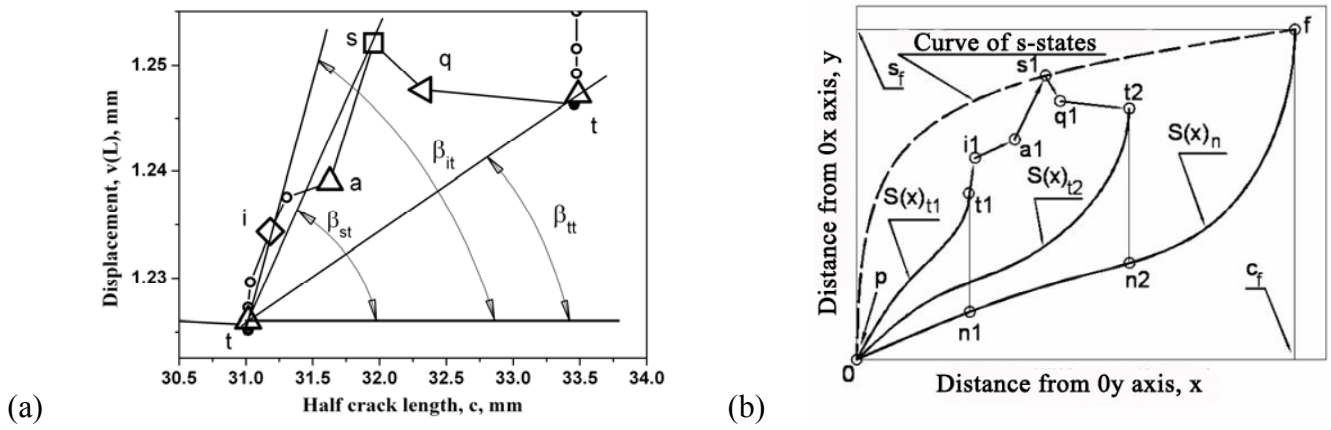

(a) (b)

Figure 9. A fragment of the test record (a) displayed earlier in Fig. 4 and schematic presentation of a transition from the one-quarter crack profile $s(x)_{t1}$ to the next profile $s(x)_{t2}$ for the spontaneously arrested crack that are shown together with two through-life fracture curves $s(x)_s$ and $s(x)_n$ related to states *s* and *n* (b).

5. General remarks

Our experimental results demonstrate that there is not worth striving for longer use of the M(T) specimen (Fig. 1a) at least in standard crack extension tests. This geometry reflects

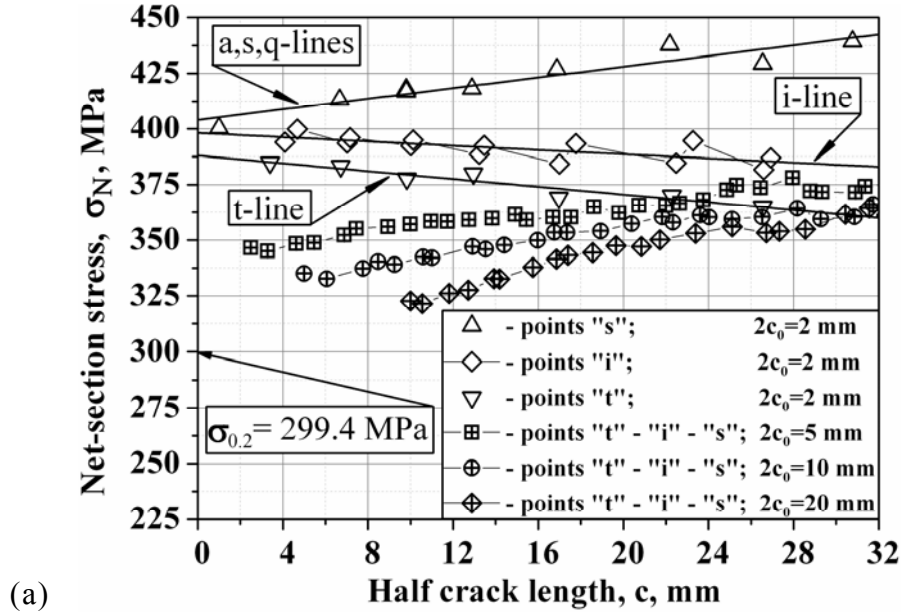

(a)

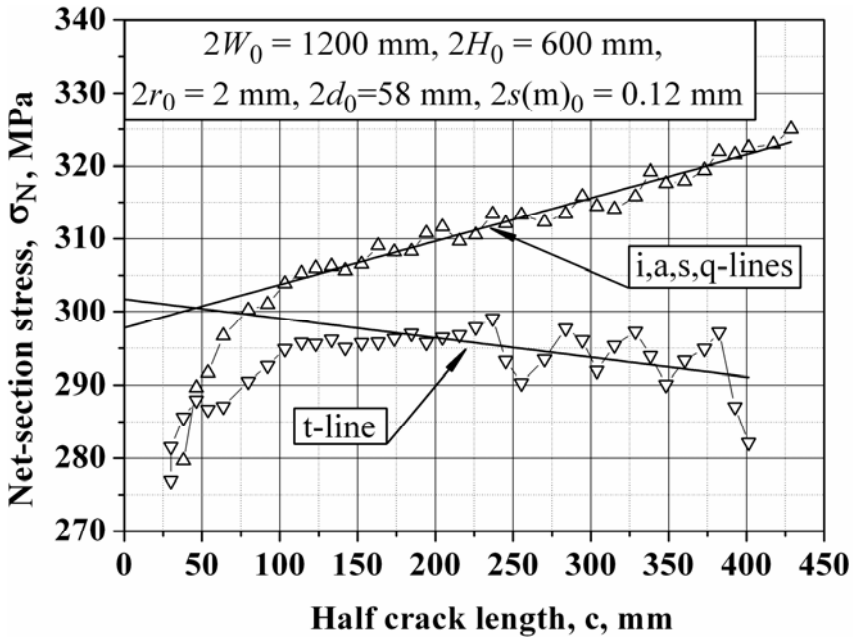

(b)

Figure 10. Experimental data for the MR(T) and MDR(T) specimens with the square PD of size $2W_0 = 2H_0 = 120$mm (a) shown together with data obtained on the MDR(T)-0.5-10.0 specimen containing the elongated stress raiser in size: $2d_0 = 58$mm, $2r_0 = 2$mm and $2s(m)_0 = 0.12$mm (b).

the out-dated incentive to apply at the horizontal PD boundaries the uniformly distributed tensile stresses. This is usually done by increasing the ratio H_0/W_0, but a price is paid in the loss of possibility to ensure realization of the fully-controllable discontinuity of the slant crack extension process. The critically important advantages of the basic MR(T) specimen result from a geometry of its PD. The smaller is the ratio H_0/W_0, the less are effects of buckling and crack extension rate on the characteristic values of the CTOA-ψ [6, 7].

As can be seen from Figs 2b and 7, the similar impact has the requirement to test the MR(T) specimens with an original stress raiser of relatively small length $2c_0 = 2r_0$. It is well known that a fatigue precrack in the M(T) specimens starts to grow by the opening mechanism and only after some advancement, comparable with the specimen thickness B_0, it propagates in the mechanism of

slanted fracture. In the MR(T) specimens, as well as in smooth tensile test specimens, nucleation of cracks and their extension both occur by one and the same mechanics of shear localisation.

Although this study is still in progress, the experimental results appear to be sufficiently significant to make the following general conclusions. It seems likely that the CTOA-ψ_c concept needs to be modified with the aim of developing the more pragmatic approach to characterization of ductile tearing resistance. In the context of this problem, the MR(T) specimen of basic geometry might be sought as an attractive alternative to geometry of the standard M(T) specimen [8-10].

Acknowledgements

I am deeply grateful to Mr. Limansky I.V. and Mr. Kravchuk, R.V. for kindly placing at my disposal the test data that were obtained in our jointly performed experimental investigation.

References

[1] V.P. Naumenko and G.S. Volkov, Assessment of plane stress tearing in terms of various crack-driving parameters, in: Fatigue and Fracture Mechanics, ASTM STP1461, S. R. Daniewicz, J. C.Newman, Jr., and K.-H. Schwalbe (Eds), West Conshohocken, PA: ASTM International, 34 (2003) 182-202.

[2] V.P. Naumenko, A.G. Atkins, Engineering assessment of ductile tearing in uniaxial and biaxial tension. Int. J. Fatique, 28 (2006) No. 5-6, 494-503.

[3] V.P Naumenko, S.V. Lenzion, I.V. Limansky, Displacement-based assessment of ductile tearing under low-constraint conditions. The Open Mechanical Engineering Journal, 2 (2008) 40-59.

[4] V.P. Naumenko, Through-life assessment of ductile tearing under low-constraint conditions, in: Proc. of 12th Int. Conf. On Fracture, Elboujdaini M., (Ed.), Ottawa, 2009, 10 pages.

[5] V.P. Naumenko, I.V Limansky, (2009), Energy-based assessment of ductile tearing in a thin-sheet aluminium alloy. Procedia Engineering, 1 (2009) issue 1, 63-66.

[6] V.P Naumenko, I.V Limansky, R.V Kravchuk, Elastic-plastic fracture under low-constraint conditions: Part I, Characteristic states of a cracked specimen. (2013), to be published in the journal Strength of Materials.

[7] V.P Naumenko, I.V Limansky, R.V Kravchuk, Elastic-plastic fracture under low-constraint conditions: Part II, Fully developed crack. (2013), to be published in the journal Strength of Materials.

[8] *E561-74*, Recommended practice for *R*-curve determination. ASTM Standard, 1974.

[9] *E2472-06*. Standard test method for determination of resistance to stable crack extension under low-constraint conditions, ASTM Standard, 2007.

[10] *ISO 22889,* Metallic materials - Method of test for the determination of resistance to stable crack extension using specimens of low constraint, International Standard, 2007.